ELSEVIER

ARTICLE INFO

Article history:
Received 15 July 2013
Received in revised form 16 October 2013
Accepted 19 October 2013
Available online 28 October 2013

1. Introduction

Floodplain sediments are suitable archives of palaeoenvironmental changes (Macklin et al., 2006; Starkel et al., 2006; Hoffmann et al., 2008; Notebaert and Verstraeten, 2010; Erkens et al., 2011). These sediments can be used to study the effects of climate fluctuations and human activities on the morpho-sedimentary and palaeohydrological evolution of rivers (Coulthard and Macklin, 2001; Kalis et al., 2003; Macaire et al., 2006). In the European mountainous and sub-mountainous fluvial archives, evidence of climatically induced palaeoenvironmental changes is well demonstrated, especially for the Last Glacial/Holocene transition (Starkel et al., 2007; Erkens et al., 2011; Turner et al., 2013) and for the Late Holocene neoglaciation (Herget, 2000; Huhmann et al., 2004; Morin et al., 2011). In addition, extensive human-induced overbank sedimentation of silty deposits and of hydro-sedimentary disturbances during the last millennium (Kalicki, 2000; Kukulak, 2003; Hoffmann et al., 2009; Gębica et al., 2013) with rapid acceleration in the 19th and 20th centuries (Owens et al., 1999; Grygar et al., 2011) has been demonstrated.

In the European context, detailed regional studies of the Holocene evolution of floodplain palaeoenvironments through dating of peat bogs, abandoned channels infill and overbank deposits has been conducted, especially in Spain (Benito et al., 2003), Great Britain (Macklin and Lewin, 1993, 2003), Germany (Hoffmann et al., 2008) and Poland (Starkel et al., 2006). In the Carpathians and their foreland, several studies in the catchments of mountainous and sub-mountainous rivers have been performed in Eastern Carpathian rivers such as the Moldova (Chiriloaei et al., 2012) and Dniester (Huhmann and Brückner, 2002; Huhmann et al., 2004; Gębica et al., 2013), and in the Western Carpathians, especially in the San (Kukulak, 2003), Vistula (Kalicki et al., 1996; Kalicki, 2000) and Wisłoka (Starkel, 1995). As for the Carpathian foreland in the Czech Republic, detailed studies were performed in the lower part of the Morava river floodplain using geochronological and geochemical methods (Kadlec et al., 2009; Grygar et al., 2010; Bábek et al., 2011).

Unlike the Western European regions that were significantly affected by humans before ~5000 cal. BP (Younger Subboreal) (Notebaert and Verstraeten, 2010), the Outer Western Carpathians (OWC) remained in semi-natural conditions with negligible human impact up to the 12th century, when the colonisation of the mountain piedmont took place (Opravil, 1974). Vast portions of the mountainous part of the region were nearly intact even up to the end of 16th century

when extensive deforestation interrelated with grazing activity (the so-called Wallachian colonisation) occurred (Kalicki, 2000; Gębica et al., 2013). Thus, floodplains in the western part of the Carpathians and their immediate foreland were one of the last European regions affected by humans. Using information from various types of fluvial archives, this paper explains how climate deterioration after the Holocene climatic optimum, and how historical human colonisation of the nearly natural mountainous environment affected the geomorphic processes within the floodplain situated in the OWC foreland (Bečva River, Czech Republic). The primary aims of our study are (i) to reveal the characteristic forms and sediments of a fluvial palaeonvironment of the Bečva River, (ii) to reconstruct the Late Holocene floodplain evolution by deciphering major river pattern changes together with aggradation and incision periods, and (iii) to analyse the impact of climate and land-use changes on the evolution of the floodplain. To understand the complexity of the spatio-temporal evolution of floodplains, a multidisciplinary approach is necessary (Morin et al., 2011; Turner et al., 2013). Therefore, geomorphological, geophysical, sedimentological and chronological analyses are used to form a complete explorative framework.

2. Regional settings

The Bečva River (catchment area = 1626 km^2) is a sub-mountainous river, the largest left tributary of the Morava River (26700 km^2) in the eastern part of the Czech Republic (Fig. 1). The river originates in the OWC at an elevation approximately 950 m a.s.l. The bedrock of the catchment is composed of the flysch formed of Cretaceous and Paleogene calcareous claystone and sandstone with isolated limestone outcrops (Menčík, 1983). This material is highly susceptible to denudation with minimum mean mechanical denudation rates varying between 2.5 and 13.4 mm ky^{-1} (Danišík et al., 2008; Baroň et al., 2010; Pánek et al., 2010). The region bears a high number of landslides and other slope deformations (Záruba, 1922; Krejčí et al., 2002; Smolková, 2011; Pánek et al., 2013a). Thus, the bedrock in the upper part of the catchment is considerably covered by Pleistocene/Holocene colluvial and landslide accumulations as well as alluvial fan deposits (Menčík, 1983). The mean longitudinal gradient of the river varies between 17.6‰ in the upper course and 2.13‰ in the studied reach. The mean annual discharge of the Bečva River in the Teplice nad Bečvou region is approximately 15.3 m^3 s^{-1} (Q_1 = 1-year flood discharge = 219 m^3 s^{-1}, Q_{50} = 799 m^3 s^{-1}). The hydrological regime of the river is controlled by melting snow and spring/summer rainfall. The present climate in the region is temperate with continental features, and the average annual rainfall and temperature in the Valašské Meziříčí region is 800 mm and 7.9 °C, respectively (Tolasz, 2007).

The study area (ca. 30 km^2) is situated in the middle reach of the Bečva River, in the foreland of the mountainous part of OWC at an elevation between 280 and 255 m a.s.l. (Fig. 1). It is formed by a wide (up to 3 km) floodplain fringed by Mid–Late Pleistocene river terraces (Macoun et al., 1965). The northern part of the valley was partly affected by Pleistocene continental glaciation during its maximum advance in the Saalian 1 (Ehlers and Gibbard, 2004). Contrary to the catchment part above the study area where the valleys are deeply incised and vast forests predominate, the valley in the studied section is wider, and crop farming, scattered forests and urbanised areas dominate. The first mention of settlement of the nearby valleys is only from the early 12th century, and colonisation of the mountainous part of the catchment took place in the 16th–17th centuries (Kalicki, 2000; Štika, 2007; Gębica et al., 2013).

3. Materials and methods

To perform detailed geomorphic mapping of the area, we conducted GPS-based geomorphic mapping with the aim of defining the extent of the active floodplain and terraces and the location of abandoned channels, in addition to selecting transects for drilling and exposures for further detailed analyses. Sequences of historical maps (in 1834, 1850, and 1877) and aerial photos (in 1955 and 2011) were analysed for reconstruction of floodplain changes since the beginning of the 19th century. The scale of the maps varies from 1:2880 (cadastre map in 1834) to

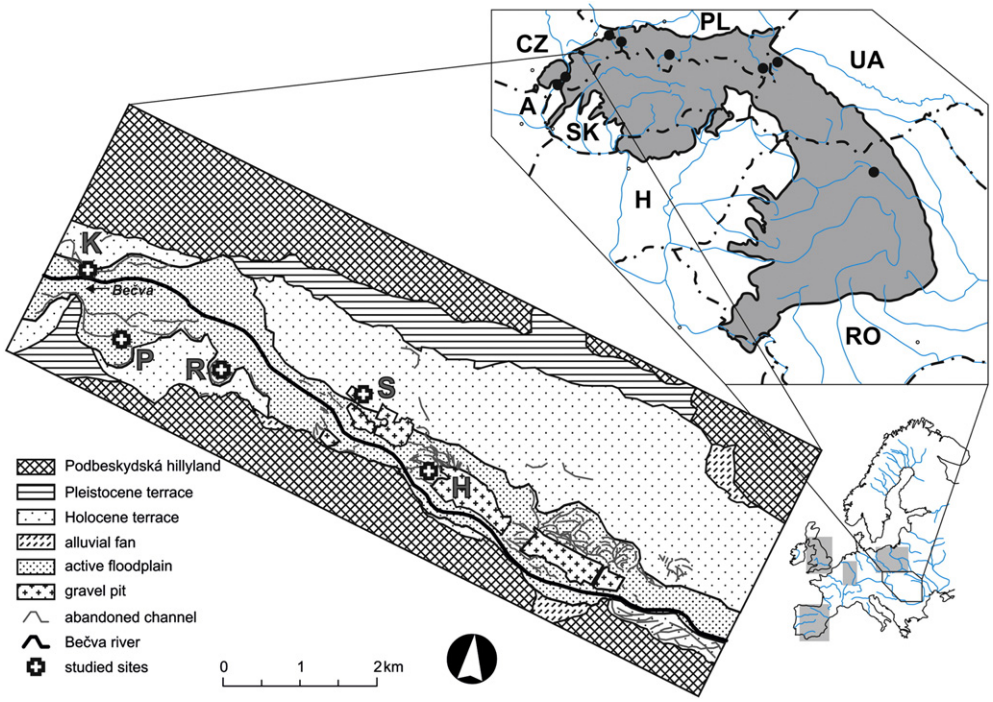

Fig. 1. Map of studied floodplain with marked discussed sites and location of studied floodplain within Europe (lower right — grey rectangles mark discussed European regions) and within Carpathians (upper right — points mark discussed Carpathian catchments). A — Austria; CZ — Czech Republic; HU — Hungary; PL — Poland; RO — Romania; SK — Slovakia; UA — Ukraine.

1:25,000 (3rd Austrian Military Survey in 1877). Land-use changes in the river catchment between the beginning of the 19th century and modern times were studied by comparing files for 77 partial cadastre areas from the years 1845, 1948, 1990 and 2000. Sedimentary facies and floodplain thickness were observed directly from 41 shallow core drillings (maximum depth 3.5 m) retrieved with a percussion sampler (Eijkelkamp®) along four transects and in two abandoned meanders. As additional information, records concerning 91 cores (max. depth 16 m) irregularly distributed over the valley provided by the Czech Geological Survey were also used. The elevation of each drilling location was measured using a total station with an accuracy of 0.5 cm. One natural (site H) and one artificial (site S) outcrop were studied in the river bank and gravel pit, respectively.

The reconstruction of the floodplain architecture between cores and/or exposures was performed using the near-surface geophysical method (Milsom, 2005). We applied an Automatic Resistivity System ARES (GF Instruments®) to gather 25 electrical resistivity tomography (ERT) profiles with a total length of approximately 3 km. Considering the contrasting conductivity of the floodplain sediments with different porosity and grain size characteristics, the ERT method is reliable for determining their extent (Gourry et al., 2003; Froese et al., 2005). Three electrode arrays (Dipole–Dipole, Wenner–Schlumberger and Wenner Alpha) with 1 m electrode spacing and a ca. 12 m depth of investigation were used (Loke, 2012). A single 150 m long shallow seismic refraction (SSR) profile was performed using the Seistronix RAS-24® system with basic survey geometry determined by the use of 11 geophones with 3 m spacing and seven seismic impact sources in the each of five geophone spreads. In addition, two perpendicular ground penetrating radar (GPR) profiles using a MALÅ Ramac X3M system with 100, 250 and 500 MHz shielded antennas and a total length of ~400 m were used to verify the ERT results.

Twenty-four organic samples (seeds, leafs, wood and charcoals) were submitted for ^{14}C AMS (accelerator mass spectrometry) dating at the Center for Applied Isotope Studies, University of Georgia (USA). The ^{14}C absolute ages were calibrated with OxCal v4.0.5 (Ramsey, 2007) using the calibration curve IntCAL09 (Reimer et al., 2009). The cal. ages are reported with the extremes of 1σ ranges. The detailed chronological constraints and sedimentation rates for the representative section H were supplemented by ^{137}Cs analysis. The ^{137}Cs activity for each 2.5 cm thick slice of the section was determined through laboratory gamma emission at 662 kEv in the Department of Geology (Palacký University, Olomouc, Czech Republic). The mass activity of ^{137}Cs was measured using a GS-320 (Exploranium Inc., Canada) laboratory gamma-ray spectrometer with a NaI (Tl) scintillation detector, 9 Bq kg^{-1} detection limit and 30 min measurement time for each sample. This analysis was complemented also by insight into the geochemical composition of the clay fraction, which was determined via X-ray fluorescence analysis (XRF) by using a PANanalytical MiniPal4.0 spectrometer with a Peltier-cooled silicon drift energy dispersive detector at the Center for Applied Isotope Studies, University of Georgia (USA).

For determination of the physical composition of key floodplain sections, we selected nine reference cores, which were sliced into 2.5 cm thick increments. The sediments were dried in the ambient atmosphere and gently crushed before analyses. The total organic content in the samples was determined by the loss of weight of a sample on ignition at 550 °C using the methodology of Heiri et al. (2001). After eliminating organic fragments, the particle size distribution was established by wet sieving for the gravel (below −1 φ) and by laser microanalysis (Malvern Mastersizer 2000®) for the sand (−1 to 4 φ), silt (4 to 8 φ) and clay (above 8 φ) (Krumbein and Sloss, 1963). We evaluated the low field mass specific magnetic susceptibility at low frequency (χ_{LF}) of each sample of the 32 cores, using an MS2 Magnetic Susceptibility Meter (Bartington Instruments®) for correlation of the studied sedimentary sections based on mineral magnetic content.

4. Results

4.1. Channel pattern change as documented by geomorphic mapping and analysis of historical maps

A geomorphological survey reveals a ca. 3 km wide floodplain fringed by 10–11 m high Middle–Late Pleistocene river terraces. The valley floor is formed by two Holocene floodplain levels at 4–5 and 2 m above the present river channel, respectively (Fig. 1). The surface of the more extensive higher floodplain level, covered by fine overbank deposits with a well-developed soil, is flattened by intensive crop farming, and thus a very limited number of small fluvial landforms (e.g., oxbows and chutes) have been preserved. This higher floodplain level is separated by a ~2 m high step from the lower floodplain level. Well-preserved oxbows (site R) with steep erosional banks and point bars were detected on the left flank of the lower floodplain level. Closer to the axis of the valley and active channel (site P), multiple deep, narrow and straight palaeochannels occur. At site H there are shallow and wide linear palaeochannels that are filled with a thick layer of overbank deposits and separated by gravel bars. The gravel bars and palaeochannels can be distinguished from the colour change of the vegetation in the aerial photos. Narrow channels of an ephemeral streams in the margin of the lower floodplain level (sites H and K) are filled with water only during the spring floods from the melting snow and when floating ice debris dams the main channel. Landform assemblages within the lower floodplain level reveal two dominant river patterns in the final stage of the floodplain evolution. The occurrence of oxbows and point bars on the outer floodplain margin proves the meandering style of the former river course. The straight, narrow and deep channels closer to the contemporary river indicate the latter-course anastomosed river pattern.

From the historical maps and aerial photos it is evident that during the 19th century, the Bečva River had, in the studied section, an anabranching pattern with gradual lateral shifting and simultaneous narrowing of the active channel belt (Fig. 2). A direct record of avulsions is present on the two versions of the cadastre map from the year 1834, where the lateral movement of the main channel of ca. 200 m during the single year is depicted. The concentration of discharge into a single channel is the main trend of the channel network development from the beginning of 20th century. The river pattern change from an anabranching system into a single, actively incising channel was accomplished in the first half of the 20th century by reinforcement of the river banks.

4.2. Geophysical dataset

After comparing our results obtained by the ERT method with the core data, four distinctive sedimentary environments were distinguished. In all 2D profiles, highly conductive (<50 Ω m) bedrock formed by claystones is overlain by a layer of gravel with variable thickness and high resistivity (150–2000 Ω m; depending on the ground water level) can be found. A relatively conductive layer of finer-grained sediment forms the floodplain surface. In this layer, two different sedimentary environments can be distinguished: deeper, linear and less resistive (10–80 Ω m) palaeochannel infill formed by clayey silts and shallower, extensive and less conductive overbank deposits (30–200 Ω m) formed by sandy silt with sand intercalations (Fig. 3).

The GPR results complement and verify the ERT measurements. It turns out that the most usable data are from the 100 MHz antenna, which reveals a prominent undulated reflector at 20–40 ns (1–2 m depth), underlain by a zone with refracted reflections and with abrupt attenuation of the signal return below 120–140 ns (5.5–6.5 m depth). The first zone corresponds to the thickness of overbank deposits indicated by boreholes. The second zone, marked by refracted reflections, indicates the thickness of *sandy gravel* facies,

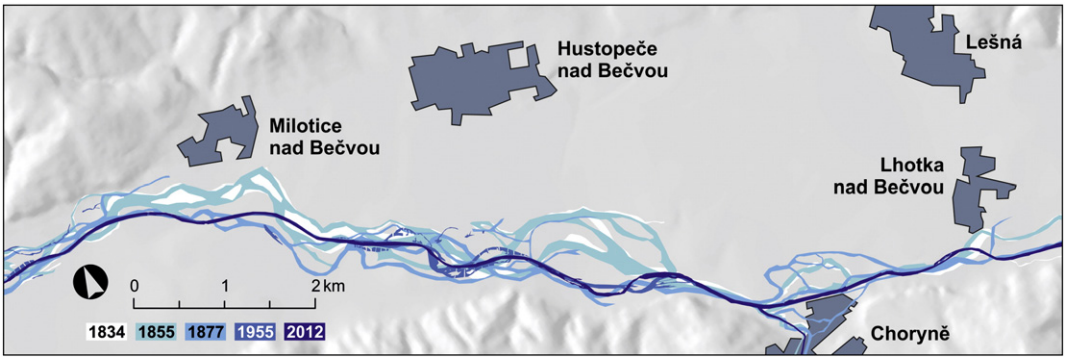

Fig. 2. River pattern as documented on historical maps and ortophotos. Note the narrowing of channel belt in the 19th century.

whereas the horizon with signal return attenuation delineates unweathered claystone bedrock.

The SSR survey data usefully complements the ERT results, especially in the zone affected by ground water, where there is a distinctive shear wave velocity horizon between unconsolidated floodplain sediments (0.3 km s^{-1}) and the weathered bedrock (1.4 km s^{-1}) occurring at the depth of 3 to 4.5 m. A second undulated seismic refractor is situated at a depth of 5–9 m and can be interpreted as a boundary between weathered (1.4 km s^{-1}) and rigid (1.9 km s^{-1}) bedrock.

4.3. Facies composition and distribution

The distribution of the lithological facies in each transect is shown in Fig. 4. The composition of the sediments within the reference cores is shown in Fig. 5. From the partial sedimentological features, nine lithological facies were identified: eight fluvial facies (*sandy gravel, sand, silty sand, sandy-silt and organic-matter poor sandy silt, silt, organic-matter poor silt and organic-matter rich silt*) and an *anthropogenic embankment*.

The *sandy gravel* facies forming the bottom layer of alluvial infill were observed in all transects and boreholes and constitutes the major part of the floodplain deposits. In the upper floodplain level, this facies also forms intercalations in finer sediments. In the *sandy gravel*, the heterometric gravel and sand fractions form more than 70% of the sediment bulk, with at least 25% gravel. The clay fraction content is negligible in this facies. The gravel fraction is mainly composed of well-rounded and rounded sandstones impregnated with limonite, with the longest axis varying from 3 to 15 cm. The *sandy gravel* facies is up to 7 m thick (site S) in the upper floodplain and 6 m thick (site H) in the lower floodplain level, where it reaches surface. The well-marked surface of this layer is highly irregular with more than 4.5 m high undulations. In the lower floodplain level, the colour of this facies is beige to grey; in the upper floodplain level, the colour is grey with rusty and black horizontal stripes. Tree trunks with diameters up to 100 cm and branches with decomposed leaves embedded in this facies can be found in the upper floodplain level. According to Miall (2006), this facies can be classified as facies Gh (clast-supported, crudely bedded gravel) and can be interpreted as element GB (gravel bars and bedforms).

The *sand* facies usually form interbedded lenses and beds 0.2 to 0.5 m thick in the *sandy gravel* facies of both the floodplain levels. In the lower floodplain level, *sand* facies form intercalations (less than 15 cm thick) in the finer sediments of infilled channels. In the upper floodplain level, laminae and crossbedding are often present in the *sand* facies. The sand fraction forms 50–80% of the total bulk of these intercalations and beds; silt and gravel fractions in total form less than 30%, and clay fractions form only an insignificant amount of the total bulk rate. The organic matter content of these facies is 5–10% in the beds in coarser sediments and less than 5% in the intercalations in channel infill. The colour of this facies is yellow to beige and streaked with orange and brown to black colour stripes and stains due to ferruginous and manganese impregnation. According to Miall (2006), these facies

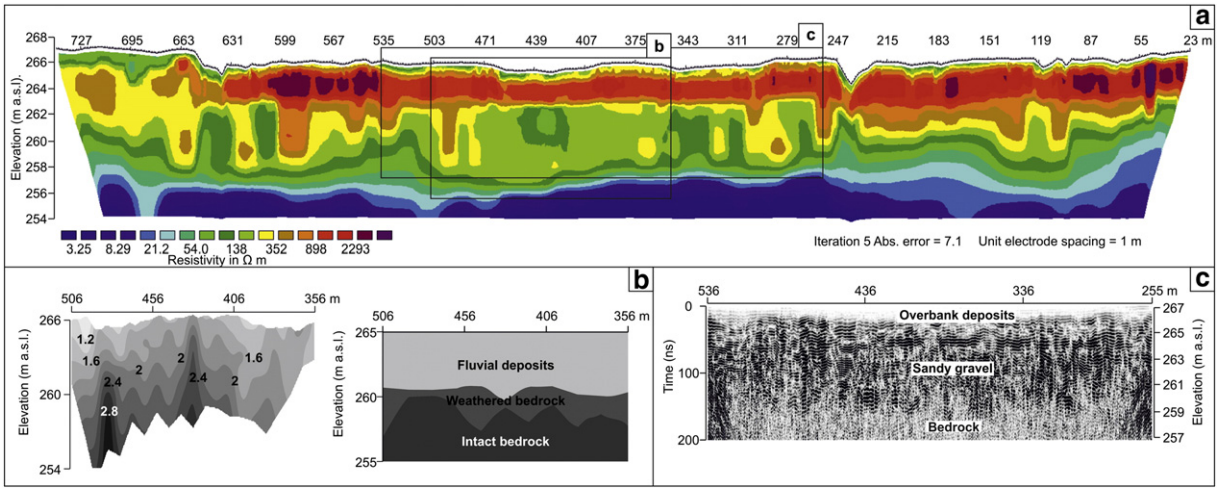

Fig. 3. Geophysical profiles of site H. The river bank is located at 0 m, and at 645 m, a step separating the upper and lower floodplain levels is located. All profiles are at the same horizontal and vertical scale. a) Electrical resistivity tomography. The ground water table is located at 264 m a.s.l. Note the lower resistivity of the overbank deposits and lower conductivity of the underlying sandy gravel. b) Shallow Seismic Refraction. Left — measured seismic velocities (km s^{-1}). Right — interpretation of sedimentary architecture. c) Ground penetrating radar — shielded 100 MHz antenna. Note the prominent reflector at the ~1 m depth (sandy gravel) and the zone of refracted reflections below ~260 m a.s.l. (rigid bedrock).

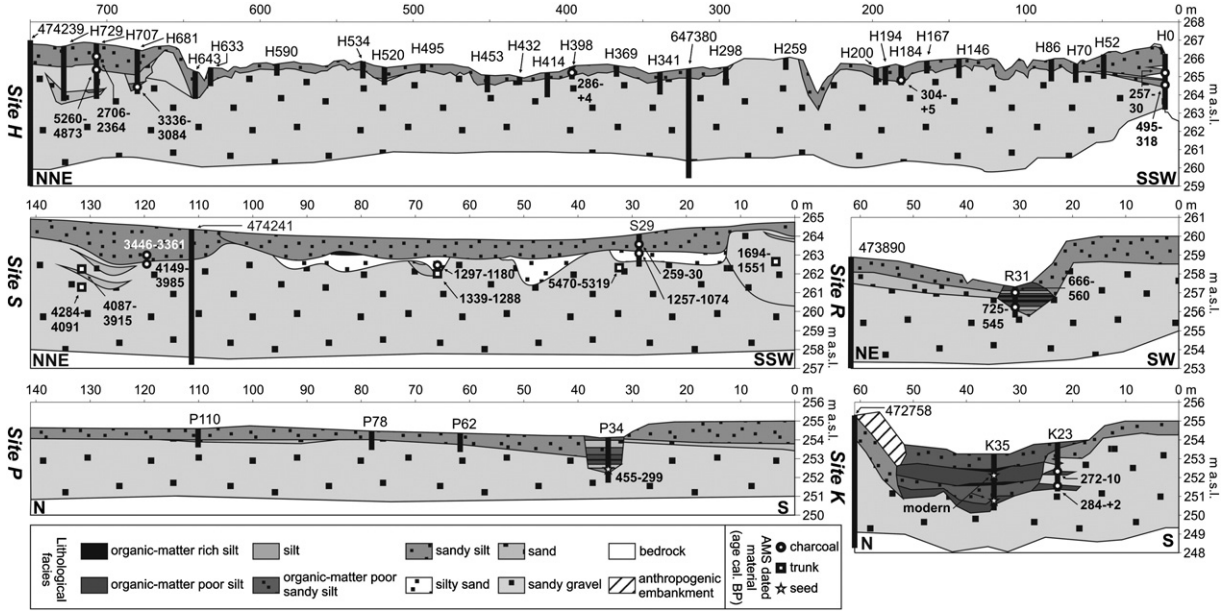

Fig. 4. Lithological transects through the studied locations with marked radiocarbon dated samples (cal. BP ± 1σ). Note the different horizontal scale in site H.

can be classified as facies Sm (sand, fine to coarse) and, excluding channel infill, can be interpreted as element CS (crevasse splay) and SB (sandy bedforms).

The *silty sand* facies are on the upper floodplain level (site S) represented as multiple ~1 m thick intercalations. These trough-like shaped greyish intercalations are arranged in one horizontal level and can be traced for hundreds of meters. The curved, concave-up erosional surface bounds the base of these facies. The contact with the superimposed overbank deposits is planar and non-erosional. More than 55% of the total bulk of this facies is formed by silt-sized fractions; the amount of the clay fraction is negligible. Abundant charcoal fragments and rare trunks and branches are embedded in this layer. On the lower floodplain level, these facies form lenses up to 60 cm thick. These facies can be classified according to Miall (2006) as facies Fl (sand, silt, mud) and interpreted as element CH (channels).

The *organic-matter poor sandy silt* and *sandy silt* facies differ in their organic matter content (10–20% and less than 10%, respectively) and dominate the fine superimposed layer of floodplain filling. On the

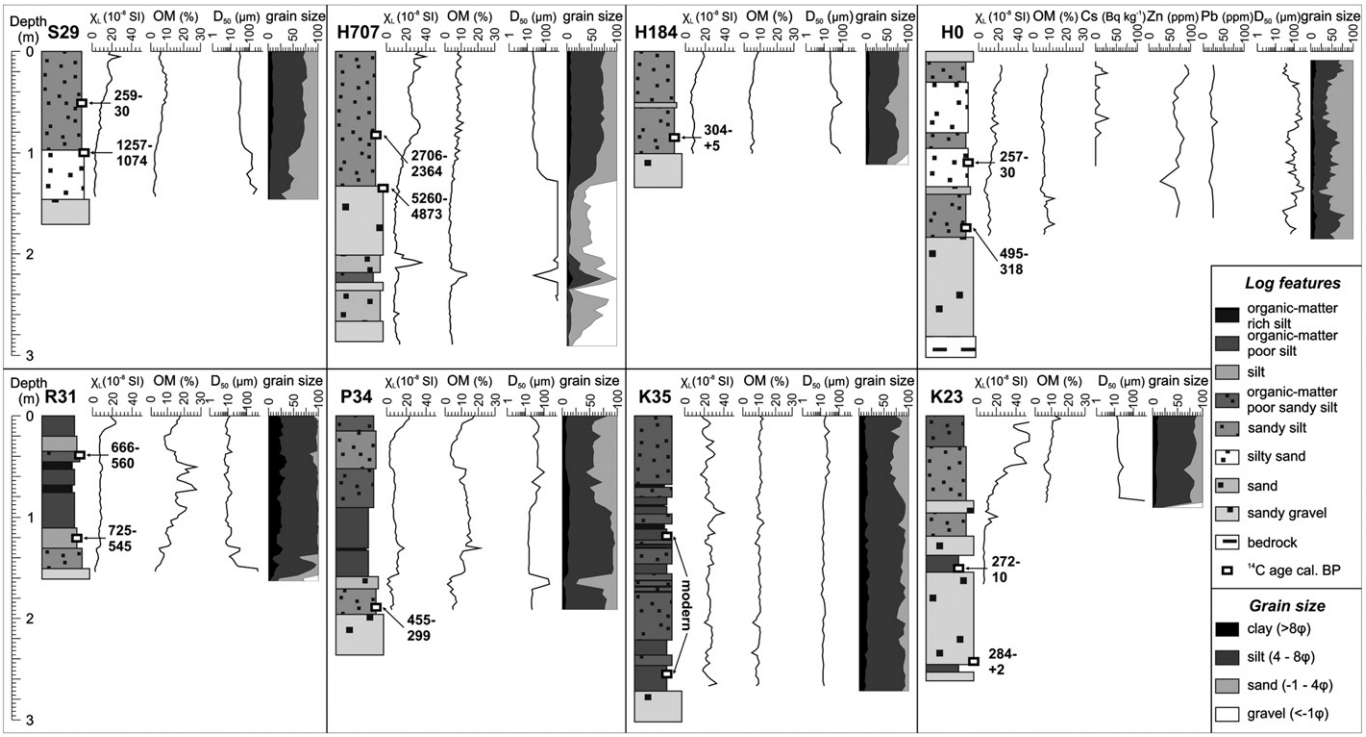

Fig. 5. Facies distribution and composition in reference cores. The grain size distribution is expressed as a percentage of the analysed fraction. χ_L — low field mass specific magnetic susceptibility at low frequency ($\times 10^{-8}$ m^3 kg^{-1}); *OM* — organic matter content; D_{50} — median grain diameter; *Cs* — ^{137}Cs mass activity; *Zn* and *Pb* — concentration of Zinc and Lead in clay fraction, respectively. For the core location, see Fig. 4.

Table 1
AMS-radiocarbon dates from the Bečva River floodplain. Calibration with IntCal09 (Reimer et al., 2009). Holocene chronozones from Mangerud et al. (1974).

Lab No.	Site	Floodplain level	Analysed material	Stratigraphic position	Depth (cm)	Surface elevation (m a. s. l.)	Age ± error (^{14}C BP)	Age (BC/AD)	Age cal.BP (±1σ)	Holocene chronozone
H1	H0	Lower	Charcoal	Bottom of overbank deposits	178	266	360 ± 20	1455–1632	495–318	Late Subatlantic
H2	H0	Lower	Charcoal	Middle of overbank deposits	112	266	90 ± 20	1693–1920	257–30	Late Subatlantic
B1	H184	Lower	Charcoal	Bottom of overbank deposits	83	265	200 ± 30	1646–1955	304–+ 5	Late Subatlantic
B12	H398	Lower	Charcoal	Bottom of overbank deposits	41	265	180 ± 20	1664–1954	286–+ 4	Late Subatlantic
B11	H681	Upper	Charcoal	Bottom of overbank deposits	195	266	3020 ± 25	−1386–−1134	3336–3084	Late Subboreal
B2	H707	Upper	Charcoal	Top of gravels	123	267	4420 ± 25	−3310–−2923	5260–4873	Atlantic/Subboreal
B10	H707	Upper	Charcoal	Middle of overbank deposits	85	267	2460 ± 25	−756–−414	2706–2364	Subboreal/Subatlantic
S14	S4	Upper	Trunk	Middle of gravels	200	265	1710 ± 20	256–399	1694–1551	Middle Subatlantic
S3	S29	Upper	Charcoal	Top of abandoned channel infill	93	264	1230 ± 20	693–876	1257–1074	Middle Subatlantic
S12	S29	Upper	Charcoal	Middle of overbank deposits	51	264	80 ± 25	1691–1920	259–30	Late Subatlantic
S6	S32	Upper	Trunk	Top of gravels	180	264	4670 ± 25	−3520–−3369	5470–5319	Late Atlantic
S2	S67	Upper	Charcoal	Middle of abandoned channel fill	130	264	1320 ± 25	653–770	1297–1180	Middle Subatlantic
S7	S67	Upper	Trunk	Bottom of abandoned channel fill	209	264	1400 ± 20	611–662	1339–1288	Middle Subatlantic
S1	S119	Upper	Charcoal	Top of gravels	189	265	3720 ± 25	−2199–−2035	4149–3985	Middle Subboreal
S10	S119	Upper	Charcoal	Bottom of overbank deposits	174	265	3170 ± 25	−1496–−1411	3446–3361	Late Subboreal
S4	S131	Upper	Trunk	Sandy intercalation in the gravel	277	265	3670 ± 25	−2137–−1965	4087–3915	Middle Subboreal
S5	S131	Upper	Trunk	Top of gravels	350	265	3800 ± 25	−2334–−2141	4284–4091	Middle Subboreal
R1	R31	Upper	Charcoal	Upper part of abandoned channel fill	39	257	650 ± 20	1284–1390	666–560	Late Subatlantic
R10	R31	Upper	Charcoal	Bottom of abandoned channel fill	121	257	680 ± 65	1225–1405	725–545	Late Subatlantic
P1	P34	Upper	Seeds	Bottom of abandoned channel fill	183	254	300 ± 25	1495–1651	455–299	Late Subatlantic
UK2	K23	Lower	Charcoal	Organic intercalation in gravels	152	254	130 ± 25	1678–1940	272–10	Late Subatlantic
UK10	K23	Upper	Charcoal	Organic intercalation in gravels	240	254	160 ± 20	1666–1952	284–+ 2	Late Subatlantic
UK3	K35	Lower	Seed	Bottom of abandoned channel fill	255	253	162.68 ± 0.41pMC	Modern	Modern	Late Subatlantic
UK4	K35	Lower	Leaf	Upper part of abandoned channel fill	119	253	132.52 ± 0.35pMC	Modern	Modern	Late Subatlantic

upper floodplain level, *sandy silt* facies form a homogenous blanket of overbank deposits up to 200 cm thick. In the lower floodplain level, this layer is discontinuous with a thickness from 20 cm on the convex floodplain segments and up to 120 cm in concave segments. The *organic-matter poor sandy silt* facies are present as 10 to 60 cm thick layers in the infill of the narrow palaeochannels on the lower floodplain level. These facies are interbedded with thin intercalations of finer sediments. In the *organic-matter poor sandy silt* and *sandy silt* facies the clay fractions are insignificant, and the sand and silt fractions largely prevail, with the latter forming more than 45% of the total bulk rate. In these layers, a large number of small charcoal fragments (less than 5 mm in diameter) are embedded. At the top of sediment pile, these layers correspond to the present soil. The *sandy silt* facies can be classified according to Miall (2006) as facies Fl and interpreted as element FF (floodplain fines). The *organic-matter poor sandy silt* facies can be interpreted as element CH(FF) — abandoned channel.

Facies mainly composed of silt fractions form layers up to 60 cm thick with sharp bounding surfaces and can be found solely on the lower floodplain where it constitutes the major part of the infill of palaeochannels. The silt fractions form more than 60% of the total bulk ratio of these facies. These deposits largely differ in their organic matter content. O*rganic-matter rich silt* contains more than 20%, *organic-matter poor silt* contains 10–20% and *silt* contains less than 10%, respectively. In oxic conditions, the prevailing colour of this facies is beige-ochre. In anoxic conditions, the colour becomes bluish-grey. These sediments are plastic when hydrated but become very rigid and brittle when desiccated. The organic matter is usually dispersed in the bulk, but it can also consist of plant fibres, leaves and grass debris, which are often arranged in distinct horizontal layers. According to Miall (2006), these facies can be classified as Fm (mud, silt) and can be interpreted as element CH(FF).

4.4. Dating and geochemical composition of floodplain sequences

Twenty-four AMS radiocarbon dates from palaeochannels, overbank deposits and underlying floodplain filling complement the sedimentological interpretations and help to establish a chronology of floodplain evolution and predominating fluvial processes. The dating results, expressed in cal. years BP related to the particular Holocene chronozones (according to Mangerud et al., 1974), are shown in Table 1.

In a ca. 150 m long bank of the gravel pit (site S) on the upper floodplain level, three trunks (*Quercus robur*) and one charcoal fragment embedded in the underlying fluvial gravels were dated to the episodes 5470–5319 and 4284–3915 cal. BP. A charcoal fragment found in the same facies on the upper floodplain level in site H was dated to 5260–4873 cal. BP. In site H, a deep and narrow channel, whose finer infill was dated to 3336–3084 cal. BP is preserved. The overbank deposits overlying these gravels were dated in sites S and H to 3446–3361 and 2706–2364 cal. BP, respectively. The distinctive *sandy gravel* accumulation in site S was dated to 1694–1551 cal. BP. Three juxtaposed palaeochannels incised into gravels were also found at this location. The charcoal and small trunk embedded in the base of first palaeochannel were dated to 1339–1180 cal. BP. The upper part of the second palaeochannel infill was dated to 1257–1074 cal. BP. Therefore, the aggradation of gravels that took place from a period before 5319 cal. BP was interrupted between 3446 and 2364 cal. BP by episodes of overbank sedimentation. The recurrence of gravel aggradation marks the following episode from 1694 to 1074 cal. BP. In the lower floodplain level, charcoal fragments in overbank deposits and infill of one oxbow and two straight deep channels were dated. The base and upper parts of the oxbow infill (site R) were dated to 725–545 and 666–560 cal. BP, respectively. The base of the channel infill in site P was dated to 455–299 cal. BP. Overbank deposits in the lower floodplain level (site H) were dated to the two phases: 495–318 cal. BP and 304–+ 5 cal. BP. In site S on upper floodplain level, overbank deposits were

dated to 259–30 cal. BP. The bottom and middle part of the ephemeral stream channel infill (site K) was in its axis dated to modern times (162.68 ± 0.41 pMC and 132.52 ± 0.35 pMC, respectively).

A layer with increased ^{137}Cs mass activity is present in the outcrop H0 (site H) in the uppermost 90 cm of the overbank deposits. Two prominent peaks were identified at a depth of 70–75 and 17.5–25 cm. The value from the deeper peak reaches mass activity of 30.1 Bq kg^{-1}, and the second peak value reaches 27.3 Bq kg^{-1}. The deeper peak is positioned in the bottom of the coarser *silty sand* intercalation and correlates with the peak in heavy metal concentrations. The upper peak correlates with decreasing low field mass specific magnetic susceptibility at low frequency (χ_{LF}) and decreasing concentrations of heavy metals.

The presence of a surface layer with increased values of χ_{LF} was proven in all reference cores. This layer is 10–100 cm thick, and χ_{LF} reaches its maxima (20–40 × 10^{-8} m^3 kg^{-1} on the upper floodplain level, 20 × 10^{-8} m^3 kg^{-1} in the lower floodplain level overbank deposits and 60 × 10^{-8} m^3 kg^{-1} in palaeochannel infill) at a depth of 10–30 cm. Overall, the χ_{LF} value depends on grain size distribution and decreases with the depth.

The heavy metal content (Pb and Zn) was studied in a natural outcrop at site H (Fig. 5). The lowest concentrations of heavy metals were recorded in the *sand* intercalation in the lower part of overbank deposits (depth 132–138 cm), and the highest concentrations were measured in the upper part of overbank deposits due to the sorption of heavy metal elements on clay particles, which form more than 10% of the total bulk ratio of this 20-cm thick layer. In particular, Zn reveals a noticeable depth maximum at 16–20 cm. The heavy metal distribution is thus largely dependent on the grain size distribution and the age of sediments. The best positive correlation can be found between the distribution of zinc, lead and χ_{LF}.

5. Discussion

5.1. Main phases and forcing factors of Late Holocene floodplain evolution

Late Holocene floodplain evolution is rarely continuous at the millennial scale (Notebaert and Verstraeten, 2010). The morpho-sedimentary dynamics and the sediment budget in catchments depend on many parameters, including the sediment yield in the catchment, the degree of slope-floodplain connection and the fluvial dynamics (Hoffmann et al., 2009; Morin et al., 2011). These parameters had a profound effect on the formation of accumulation and incision phases and varied in space and time. According to the distribution of the lithological facies and dating, six phases of fluvial dynamics were identified. These phases are numbered 1 to 6 from the oldest to the most recent and correspond either to an accumulation phase (marked with suffix A) or to an incision phase (marked with suffix I). The accumulation units are composed of one or several of the nine defined lithological facies.

The remnants of Pleistocene terrace fringes the studied floodplain 11–12 m above the present channel (Tyráček, 1963; Macoun et al., 1965). The lack of dated sediments from the first half of the Holocene suggests that some major incision episode took place, most likely in the early Atlantic. This type of massive incision indicates efficient soil protection by dense vegetation and high water discharge (Morin et al., 2011), which is consistent with the reconstructed vegetation of temperate deciduous forests that covered the Atlantic central European lowlands (Opravil, 1974; Notebaert and Verstraeten, 2010).

The oldest accumulation, phase 1A (Fig. 6), is marked by deposition of up to a 7 m thick sedimentary unit formed by *sandy gravel* facies with the presence of sparse tree trunks and charcoal fragments. The charcoal fragment and trunk embedded in the uppermost layer of this sedimentary unit in site S postdate the accumulation phase to 4149–3985 and 4087–3915 cal. BP, respectively. The trunks embedded in the lower parts of this sedimentary unit were dated to 5470–5319 and 4284–4091 cal. BP. The charcoal fragment found in this sedimentary unit in site H was dated to 5260–4873 cal. BP and supports these results. These deposits were marked as gravel bars and/or longitudinal bedforms and point to a braided fluvial system (Reineck and Singh, 1980; Miall, 2006). Analogical sediments were described from the lower parts of the Bečva and Morava River catchments (Havlíček, 2008; Vít et al., 2009). The climate deterioration that took place after the Holocene climatic Optimum (Wanner et al., 2008; Notebaert and Verstraeten, 2010) (Fig. 6) caused increased erosion and accelerated slope deformation to take place (Pánek et al., 2013b) in the upper parts of the catchment. Although many settlements were described in the Morava gate (Šebela et al., 2007), almost no Eneolithic artefacts have been found in the studied area, indicating very limited human impact on the environment (Schenk, 2004). The sparse charcoal fragments may originate from the slash-and-burn agriculture technique (Rodenburg et al., 2003).

The 1–2 m thick extensive blanket consisting of *sandy silt* facies was preserved on the upper floodplain level and marks phase 2A (Fig. 6). The onset and termination of this phase was dated to 3446–3361 and 2706–2364 cal. BP, respectively. The occurrence of the narrow, deep channel with infill bottom dated to this period (3336–3084 cal. BP) suggests an anastomosed channel pattern and overbank sedimentation as a prevailing process (Brierley and Fryirs, 2005). The earlier onset of overbank sedimentation in the lower parts of the Morava River catchment (4244–3914 cal. BP) (Vít et al., 2009) is most likely a result of intensified deforestation and crop farming in that area (Podborský et al., 1993). The population density in the Bečva River catchment is considered to be even lower than in the preceding Eneolithic phase (Opravil, 1974; Čižmářová, 2004).

During the phase 3IA (Fig. 6), the ~2 m thick *sandy gravel* sedimentary unit was formed and multiple shallow and wide abandoned active channels were infilled with *silty sand*. Due to the partial absence of unit 2A, this phase was erosional in the early stages. The sedimentary units of this phase are preserved in a ~100 m wide discontinuous strip forming the inner fringe of the upper floodplain level (sites S and H). The trunks embedded at the depth of 200 cm in the gravel bar postdate the onset of this phase to 1694–1551 cal. BP; three channel infill samples were dated to 1339–1074 cal. BP. These sedimentary units point to the recurrence of a braided river pattern and gravel aggradation in the middle Subatlantic (Roman Times, Dark Ages and Early Middle Ages) and a later decrease in the discharge and/or sediment yield of the sub-catchments (Brierley and Fryirs, 2005). Colder and more humid climate caused the decrease of the tree line in the OWC (Ralska-Jasiewiczowa, 1980), and many older landslides in the studied catchment were reactivated during this phase (Pánek et al., 2013b). Literally no archaeological artefacts from this period were found in the studied catchment (Šebela et al., 2007), contrary to the other European regions that have been largely affected by crop farming and human-induced deforestation (Dotterweich, 2008).

The considerable incision that formed a rudimentary planar surface of the lower floodplain level occurred in phase 4I (Fig. 6). Several infilled palaeomeanders with developed point bars (e.g. site R) are located in the outer fringe of the lower floodplain level, whereas they are laterally cut into the upper floodplain level, indicating that the prevailing process was lateral erosion (sensu Gordon et al., 2004). The base of its infill (725–545 cal. BP) postdates this major incision phase that created the new valley channel zone. Kadlec et al. (2009) described a similar period of lateral erosion caused by increased fluvial activity during the 10th century in the lower part of the Morava River catchment. Human settlements in the studied area formed only a few enclaves in the vast forests (Opravil, 1974).

The extensive 20 to 180 cm thick *sandy silt* sedimentary unit marks phase 5A (Fig. 6). An abandoned meander in site R was infilled between 725–545 cal. BP and 666–560 cal. BP. The base of the straight deep and narrow channel infill at site P was dated to 455–299 cal. BP. Overbank deposits in sites H, K, S are dated from 495 to +5 cal. BP. Infill from

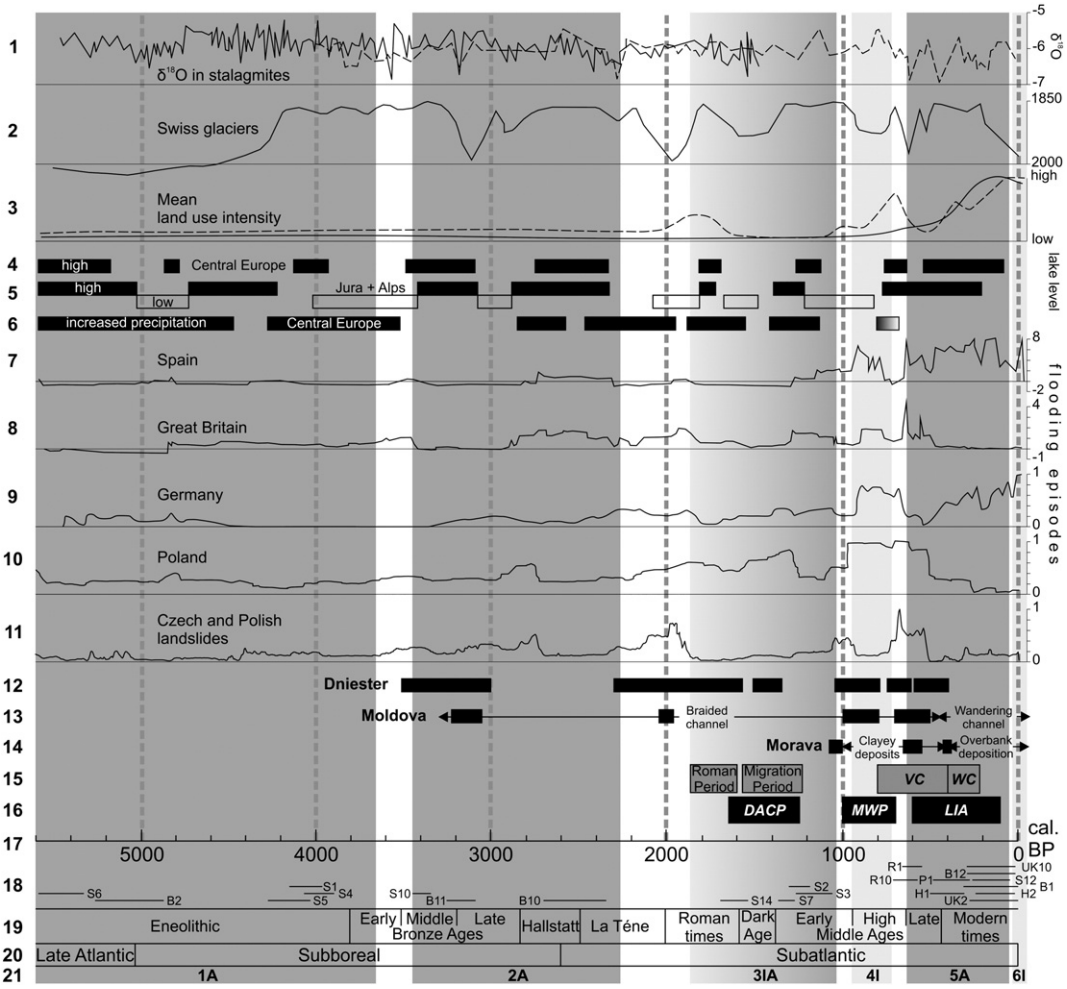

Fig. 6. Synthesis of past climate, land-use intensity and hydrological events from Late Atlantic to present day. 1) $\delta^{18}O$ record from stalagmites AH-1 (solid line) and B7-7 (dashed line) (Sauerland, Germany) from Niggemann et al. (2003). 2) Swiss glacier length variations from Glaser et al. (2005). 3) Dashed line: mean intensity of land use (fields, grassland and forests) in central Europe (Dotterweich, 2008), and estimated intensity of land use in studied catchment (solid line, own studies). 4) Phases with increased lake-levels in central Europe from Magny (2004). 5) Phases of lake-level changes in Jura and Swiss Alps from Magny (1993). 6) Precipitation trends in central Europe from Jäger (2002). 7), 8), and 10) Probability difference curve (PDC) of radiocarbon dates associated with major flooding episodes in Spain (7), Great Britain (8) and Poland (10) from Macklin et al. (2006). 9) Simplified cumulative probability function (CPF) of floodplain radiocarbon ages in Germany from Hoffmann et al. (2008). 11) Normalised probability density curve of the Czech and Polish landslide events (Alexandrowicz, 1993; Margielewski, 1997, 1998, 2001, 2003, 2006; Alexandrowicz and Alexandrowicz, 1999; Margielewski and Kovalyukh, 2003; Hradecký et al., 2004, 2007; Baroň, 2007; Smolková et al., 2008; Margielewski et al., 2010, 2011). 12) Periods with increased fluvial activity in the Upper Dniester River from Gębica et al. (2013). 13) Periods with increased fluvial activity and prevailing river pattern in the River Moldova (Romania) from Chiriloaei et al. (2012). 14) Periods with increased fluvial activity and prevailing deposition type in the lower part of Morava River catchment from Kadlec et al. (2009). 15) Major events in land-use intensity (VC — Colonisation of Bečva River valley, WC — Wallachian colonisation of Carpathian ridges). 16) Major climatic anomalies (DACP — Dark Ages Cold Period, MWP — Mediaeval Warm Period, LIA — Little Ice Age). 17) Timeline in cal. BP (before 1950). 18) Radiocarbon dated samples (cal. BP $\pm$ 1σ) (this study). 19) Prehistorical and historical periods in Eastern Moravia (Podborský et al., 1993). 20) Climatic Holocene phases from Mangerud et al. (1974); dark grey rectangles indicate the accumulation phases, and the light grey rectangles indicate the incision phases. 21) Phases of fluvial dynamics in the Bečva River (this study).

an ephemeral stream channel in site K is dated to modern times. These results indicate an equilibrium state without significant erosion or accumulation and a relatively stable anastomosed river pattern (sensu Nanson and Croke, 1992) from 725–545 to 455–299 cal. BP (Late Middle Ages). The abrupt onset of overbank sedimentation before 495–318 cal. BP terminated this equilibrium. Noticeable wide and shallow linear depressions on the erosional surface of sedimentary unit 1A indicate the presence of the laterally unstable wide belt of wandering channels in this phase. This narrowing belt is depicted on historical maps from the 19th century. The equilibrium state can be interpreted as a result of higher discharge (Gregory, 1987) and increased soil erosion that balanced the precedent incision phase. The higher discharge is most likely associated with ongoing climate deterioration (Bell and Walker, 2005; Dotterweich, 2008; Notebaert and Verstraeten, 2010), and the soil erosion is associated with the early phase of catchment colonisation. The colonisation connected with crop farming and deforestation of the river valley started in 12th century (the first settlements are mentioned not earlier than 1174 AD — Milotice nad Bečvou). The abrupt onset of overbank sedimentation (before 495–318 cal. BP) and the transition from an anastomosed to a wandering river channel correlates with the Wallachian colonisation, which gradually reached the mountains in the studied catchment from the 15th to 17th centuries (Štika, 2007). The charcoal burning and sheep grazing on the mountain ridges caused increased erosion of higher sediment yields from the slopes (Kukulak, 2000, 2003). These washed-out fine-grained sediments were initially deposited in the form of overbank sediments (Brierley and Fryirs, 2005). The abundant charcoal fragments originated in the extensive charcoal production in the area (Kukulak, 2000), and sparse *sand* intercalations can be interpreted as deposits of crevasse splays (Miall, 2006; Kadlec et al., 2009; Grygar et al., 2010). The gradual increase in heavy metal concentrations and χ_{LF} in the uppermost 120 cm of overbank deposits (H0) can be attributed to the increased industrial pollution of the 20th century (Grygar et al., 2011). Charcoal embedded at a depth of 112 cm and dated to 257–30 cal. BP support these

results. The 90 cm thick layer with increased ^{137}Cs mass activity is most likely the result of nuclear testing since 1950s AD (Kadlec et al., 2009). Two prominent peaks were identified at a depth of 70–75 and 17.5–25 cm. The deeper peak is positioned in the bottom of a coarser *silty sand* intercalation and can be assigned to a maximum in nuclear weapon testing in the years 1963 and 1964 (Nehyba et al., 2011; Sedláček et al., 2013). The position of the deeper peak approximately coincides with the peak in heavy metal concentrations and can be interpreted as a deposit of major floods that washed a higher amount of pollutants from the catchment in 1966 and 1970 AD (Brázdil et al., 2005). In addition, the release of heavy metals into the environment was very intense in the 1960s and 1970s due to higher industrial production in the former Czechoslovakia (Novák et al., 2003; Sedláček et al., 2013). The upper peak correlates with decreasing χ_{LF} and concentrations of heavy metals and was interpreted as atmospheric fallout deposits from the Chernobyl nuclear power plant accident in 1986 AD (Wildi et al., 2004; Bábek et al., 2011; Nehyba et al., 2011; Sedláček et al., 2013). The maximal values were not so high (cf. Bábek et al., 2008) in the outcrop H0 because the distribution of ^{137}Cs in Moravia was not uniform. The minor above-mentioned decrease in the concentration of heavy metals in the uppermost 20-cm thick layer is most likely a result of use of unleaded fuel and termination (after year 2000) of some industrial plants in the last 25 years. Similar results were described in other studies from south Moravia (Bábek et al., 2008; Kadlec et al., 2009). To summarise, the land-use changes after ~800 cal. BP induced major change in the morpho-sedimentary dynamics of the studied catchment and, for the first time, superseded climatic forcing factors.

The recent phase 6I (Fig. 6) is characterised by transition from wandering to a single vertically incised channel. This change is most likely the result of intensive reforestation (Fig. 7) and the anthropogenic modification of river geometry in the 20th century (Hrádek, 2005). Due to vertical incision, the lower floodplain level is flooded now only during major flooding episodes (discharge > Q_{20}). However, parts of the upper floodplain level were flooded during the catastrophic flood in 1997 AD (>Q_{100}) (Brázdil et al., 2005).

5.2. Specifics of Late Holocene evolution of rivers in Czech part of OWC

The Bečva River catchment exhibits similar evolutionary phases to many European catchments up to the ~800 cal. BP (Mediaeval Warm Period) (Kalicki, 2000; Macklin et al., 2006; Starkel et al., 2006; Hoffmann et al., 2008; Kalicki et al., 2008; Chiriloaei et al., 2012; Gębica et al., 2013). In the Late Atlantic, a widespread episode of cooler and wetter climate (Magny et al., 2006) affected Central Europe, and the episodes of increased precipitation lasted to the Middle Subboreal (Jäger, 2002). A major Late Subboreal flooding phase described in Spain, Great Britain and Poland corresponds with the North Atlantic ice rafting debris record (Macklin et al., 2006), thus indicating major climatic fluctuation in the Euro-Atlantic sector. The overbank sediments deposited in the Subboreal in Polish (Kalicki, 2000) and German (Notebaert and Verstraeten, 2010) catchments indicate the increased soil erosion caused by the increased precipitation (Jäger, 2002). The increased lake levels in Central Europe (Magny, 2004) and in the Jura and Swiss Alps (Magny, 1993) prove this wetter episode. Flooding episodes at ~2000–1650 cal. BP (during Roman Period) are ascribed to deforestation and crop farming (Klimek, 2002; Zygmunt, 2004; Notebaert and Verstraeten, 2010), but after ~1650 cal. BP (during the following settlement regression and forest restoration in Dark Ages Cold Period) to an increase in precipitation (Dotterweich, 2008). During this phase, the Swiss glaciers were advancing (Glaser et al., 2005). The colder climate (Dotterweich, 2008) and increased precipitation (Jäger, 2002) led to increased lake levels (Magny, 2004). Contrary to the increasing population of other European regions (Huhmann et al., 2004; Dotterweich,

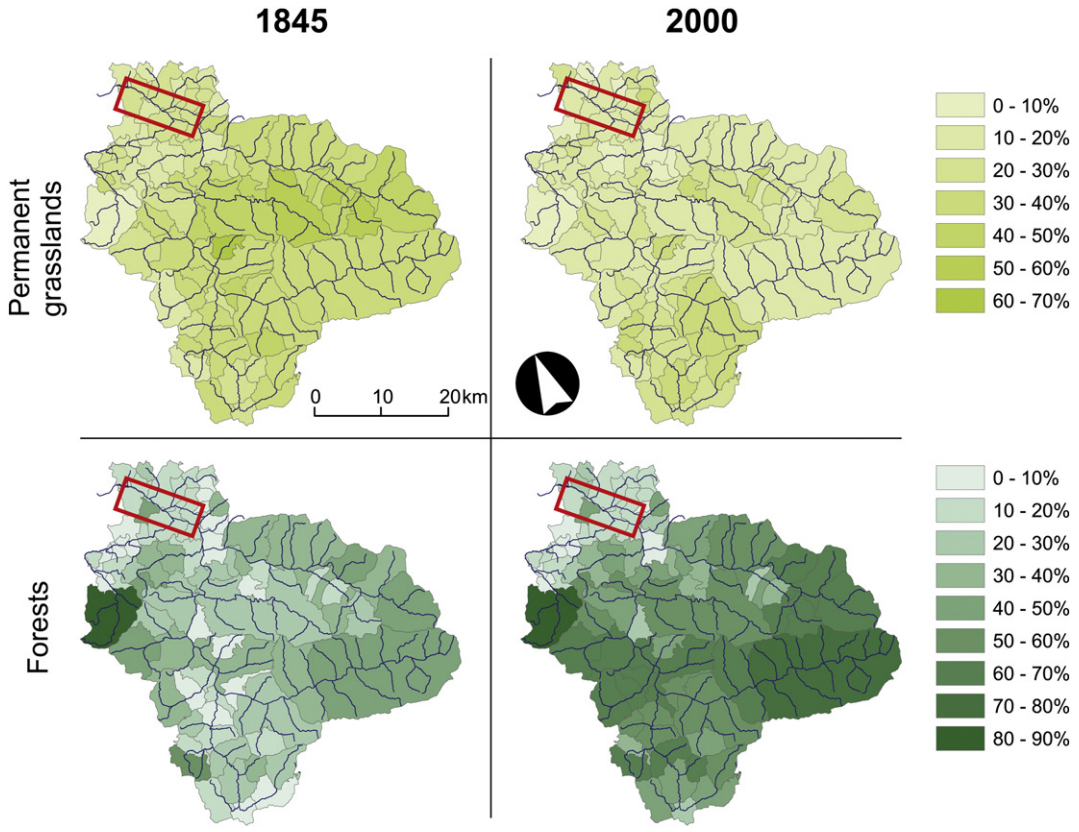

Fig. 7. Land-use of cadastre areas in the studied catchment in the years 1845 and 2000. Permanent grasslands: meadows + pastures. The rectangle marks the studied floodplain. Note the major recurrence of forests and woodlands at the expense of meadows and pastures.

2008; Notebaert and Verstraeten, 2010) with intensified land-use during the Roman Period (Klimek, 2002; Erkens et al., 2011), the studied catchment was generally uninhabited and vastly forested (Opravil, 1974; Podborský et al., 1993; Šebela et al., 2007). This evolution of the two contrasting environments suggests a major climatic impact (Huhmann et al., 2004) and only minor human-induced amplification of climate deterioration from ~1600 to 1200 cal. BP (Dark Ages Cold Period) in Central Europe.

From 1000 to 700 cal. BP the Bečva River laterally eroded its older deposits. This phase took place during the Mediaeval Warm Period (Macklin et al., 2006) with gradual change towards more oceanic features and higher temperature (Lamb, 1995; Dotterweich, 2008). During this period, the major part of the European catchments were affected by important aggradation phases (Kalicki, 2000; Macklin et al., 2006; Kalicki et al., 2008; Chiriloaei et al., 2012; Gębica et al., 2013). In contrast to other European catchments that were largely affected by intensive crop farming during this phase (Dotterweich, 2008), the studied catchment was at the very onset of its colonisation (Štika, 2007). Therefore, in the major part of Europe, human-induced aggradation prevailed over climatically induced incision in the lower parts of the catchments, whereas the evolution of the Bečva River floodplain was still controlled by natural-forcing factors.

The OWC were affected by mountainous, so called "Wallachian" colonisation after the 15th century (Kukulak, 2000, 2003; Štika, 2007). This immense anthropogenic impact on the natural environment led to massive overbank deposition (Kalicki, 2000; Huhmann et al., 2004; Chiriloaei et al., 2012; Gębica et al., 2013) and suppressed the effect of decreased temperature, cooler and wetter winters and increased the storminess of the Little Ice Age (Bell and Walker, 2005; Dotterweich, 2008; Notebaert and Verstraeten, 2010). The overbank deposition in the lower parts of Morava River floodplain started as early as in the 11th century (Kadlec et al., 2009) and is ascribed to anthropogenic forest clearings in those parts of the Morava River catchment. Kadlec et al. (2009) related the coarsening of deposits after 1550 AD to higher discharges, which are attributed to the Little Ice Age. Grygar et al. (2011) described two changes in Morava River channel structure in the 13th and at the end of 16th centuries: changes that these authors suggested were related to the climatic extremes rather than to intensified land-use in the catchments of tributaries. These interpretations contrast with the forcing factors of the evolutionary phases of the Bečva River, which is one of the largest tributaries of the Morava River.

The recent vertical cutting is a result of reforestation and massive anthropogenic influence on the active channel (Hrádek, 2005). The anthropogenic intervention consists of the channel straightening, major reinforcement of the banks, building of the dams in the upper parts of the sub-catchments and building of the weirs along the river course. A similar vertical incision dated to the last century has been described from a Carpathian sub-mountainous region where the reforestation on the abandoned pastures occurred (Huhmann et al., 2004; Chiriloaei et al., 2012).This evolutionary phase also is in direct contrast to increases in the sedimentation rate during the last 50 years in the Morava River floodplain described as being a response to intensive agriculture by Kadlec et al. (2009).

6. Conclusions

The Late Holocene evolution of the studied floodplain is generally characterised by gradual aggradation with a short incision phase during the 10th century. The late colonisation of the upper part of the Bečva River catchment preserved this part of the OWC in semi-natural conditions up to the ~800 cal. BP. This unique lack of human-induced changes led to the natural evolution of the floodplain with climate fluctuations serving as the only forcing factor. The abrupt land-cover changes during the colonisation of mountain ridges in the 16th and 17th centuries caused the major silty overbank deposition. In the 20th century, reforestation of the OWC caused significant vertical incision of the active channel; and overbank sedimentation is now limited only to the major flooding episodes.

Acknowledgments

References

Alexandrowicz, S.W., 1993. Late Quaternary landslides at eastern periphery of the National Park of the Pieniny Mountains, Carpathians, Poland. Stud. Geol. Pol. 192, 209–225.
Alexandrowicz, S.W., Alexandrowicz, Z., 1999. Recurrent Holocene landslides: a case study of the Krynica landslide in the Polish Carpathians. The Holocene 9, 91–99.
Bábek, O., Hilschnerová, K., Nehyba, S., Zeman, J., Faměra, M., Franců, J., Holoubek, I., Machát, J., Klánová, J., 2008. Contamination history of suspended river sediments accumulated in oxbow lakes over the last 25 years. J. Soils Sediments 8, 165–176.
Bábek, O., Faměra, M., Hilscherová, K., Kalvoda, J., Dobrovolný, P., Sedláček, J., Machát, J., Holoubek, J., 2011. Geochemical traces of flood layers in the fluvial sedimentary archive; implications for contamination history analyses. Catena 87, 281–290.
Baroň, I., 2007. Results of radiocarbon dating of deep-seated landslides in the area of Vsetín and Frýdek–Místek districts. Geol. výzk. Mor. Slezsku 14, 10–12.
Baroň, I., Baldík, V., Fiferová, M., 2010. Preliminary assessment of a recent denudation rate of the Flysch Belt of Outer West Carpathians — Case study: Bystřička River catchments in Vsetínské Hills. Geol. výzk. Mor. Slezsku 17, 10–13.
Bell, M., Walker, M., 2005. Late Quaternary Environmental Change. Pearson/Prentice Hall, Harlow.
Benito, G., Sopeña, A., Sánchez-Moya, Y., Machado, M.J., Pérez-González, A., 2003. Palaeoflood record of the Tagus River (central Spain) during the Late Pleistocene and Holocene. Quat. Sci. Rev. 22, 1737–1756.
Brázdil, R., Dobrovolný, P., Elleder, L., Kakos, V., Kotyza, O., Kvetoň, V., Macková, J., Müller, M., Štekl, J., Tolasz, R., Valášek, H., 2005. Historical and recent floods in the Czech Republic. Masaryk University and Czech Hydrometeorological Institute, Brno.
Brierley, G.J., Fryirs, K.A., 2005. Geomorphology and River Management: Applications of the River Styles Framework. Blackwell Publishing, Malden.
Chiriloaei, F., Rădoane, M., Perşoiu, I., Popa, I., 2012. Late Holocene history of the Moldova River Valley, Romania. Catena 93, 64–77.
Čižmářová, J., 2004. Encyklopedie Keltů na Moravě a ve Slezsku. Libri, Praha.
Coulthard, T., Macklin, M., 2001. How sensitive are river systems to climate and land-use changes? A model-based evaluation. J. Quat. Sci. 16, 347–351.
Danišík, M., Pánek, T., Matýsek, D., Dunkl, I., Frisch, W., 2008. Apatite fission track and (U–Th)/He dating of teschenite intrusions gives time constraints on accretionary processes and development of planation surfaces in the Outer Western Carpathians. Z. Geomorphol. 52, 273–289.
Dotterweich, M., 2008. The history of soil erosion and fluvial deposits in small catchments of central Europe: deciphering the long-term interaction between humans and the environment — a review. Geomorphology 101, 192–208.
Ehlers, J., Gibbard, P.L. (Eds.), 2004. Quaternary Glaciations — Extent and Chronology: Part I: Europe. Elsevier, Amsterdam.
Erkens, G., Hoffmann, T., Gerlach, R., Klostermann, J., 2011. Complex fluvial response to Lateglacial and Holocene allogenic forcing in the Lower Rhine Valley (Germany). Quat. Sci. Rev. 30, 611–627.
Froese, D.G., Smith, D.G., Clement, D.T., 2005. Characterizing large river history with shallow geophysics: middle Yukon River, Yukon Territory and Alaska. Geomorphology 67, 391–406.
Gębica, P., Starkel, L., Jacyšyn, A., Krąpiec, M., 2013. Medieval accumulation in the Upper Dniester river valley: the role of human impact and climate change in the Carpathian Foreland. Quat. Int. 293, 207–218.
Glaser, R., Ammann, B., Brauer, A., Heiri, O., Jacobeit, J., Lotter, A.F., Luterbacher, J., Maisch, M., Magny, M., Pfister, C., Tinner, W., Veit, H., Wanner, H., 2005. Palaeoclimate within the River Rhine catchment during Holocene and historic times. Erdkunde 59, 251–275.
Gordon, N.D., McMahon, T.A., Finlayson, B.L., Gippel, C.J., Nathan, R.J., 2004. Stream Hydrology, An Introduction for Ecologists. Wiley, Chichester.
Gourry, J.C., Vermeersch, F., Garcin, M., Giot, D., 2003. Contribution of geophysics to the study of alluvial deposits: a case study in the Val d'Avaray area of the River Loire, France. J. Appl. Geophys. 54, 35–49.
Gregory, K.J., 1987. River channels. In: Gregory, K.J., Walling, D.E. (Eds.), Human Activity and Environmental Processes. Wiley, Chichester, pp. 207–235.
Grygar, T., Světlík, I., Lisá, L., Koptíková, L., Bajer, A., Wray, D.S., Ettler, V., Mihaljevič, M., Nováková, T., Koubová, M., Novák, J., Máčka, Z., Smetana, M., 2010. Geochemical tools for the stratigraphic correlation of floodplain deposits of the Morava

River in Strážnické Pomoraví, Czech Republic from the last millennium. Catena 80, 106–121.
Grygar, T., Nováková, T., Mihaljevič, M., Strnad, L., Světlík, I., Koptíková, L., Lisá, L., Brázdil, R., Máčka, Z., Stachoň, Z., Svitavská-Svobodová, H., Wray, D.S., 2011. Surprisingly small increase of the sedimentation rate in the floodplain of Morava River in the Strážnice area, Czech Republic, in the last 1300 years. Catena 86, 192–207.
Havlíček, P., 2008. Flood plain of the Dyje River between Lednice and Bulhary. Geoscience Research Reports for 2007. 89–90.
Heiri, O., Lotter, A.F., Lemcke, G., 2001. Loss on ignition as a method for estimating organic and carbonate content in sediments: reproducibility and comparability of results. J. Paleolimnol. 25, 101–110.
Herget, J., 2000. Holocene development of the River Lippe valley, Germany: a case study of anthropogenic influence. Earth Surf. Process. Landf. 25, 293–305.
Hoffmann, T., Lang, A., Dikau, R., 2008. Holocene river activity: analysing ^{14}C-dated fluvial and colluvial sediments from Germany. Quat. Sci. Rev. 27, 2031–2040.
Hoffmann, T., Erkens, G., Gerlach, R., Klostermann, J., Lang, A., 2009. Trends and controls of Holocene floodplain sedimentation in the Rhine catchment. Catena 77, 96–106.
Hradecký, J., Pánek, T., Břízová, E., 2004. Contribution to the geomorphology and the age of the selected slope deformations in the area of Slezské Beskydy Mts. and Jablunkovská Brázda Furrow. Geografie 109, 289–303.
Hradecký, J., Pánek, T., Klimová, R., 2007. Landslide complex in the northern part of the Silesian Beskydy Mountains (Czech Republic). Landslides 4, 53–62.
Hrádek, M., 2005. Origin of meandering-thalweg channel on the Bečva river after flood in July 1997. In: Rypl, J. (Ed.), Geomorfologický sborník 4. Jihočeská universita v Českých Budějovicích, České Budějovice, pp. 51–54.
Huhmann, M., Brückner, H., 2002. Holocene terraces of the Upper Dnister. Fluvial morphodynamics as a reaction to climate change and human intrusion. Z. Geomorphol. N.F. Suppl. 127, 67–80.
Huhmann, M., Kremenetski, K.V., Hiller, A., Brückner, H., 2004. Late Quaternary landscape evolution of the Upper Dnister valley, Western Ukraine. Palaeogeogr. Palaeoclimatol. Palaeoecol. 209, 51–71.
Jäger, K.D., 2002. Oscillations of the water balance during the Holocene in interior Central Europe — features, dating and consequences. Quat. Int. 91, 33–37.
Kadlec, J., Grygar, T., Světlík, I., Ettler, V., Mihaljevič, M., Diehl, J.F., Beske-Diehl, S., Svitavská-Svobodová, H., 2009. Morava River floodplain development during the last millennium, Strážnické Pomoraví, Czech Republic. The Holocene 19 (3), 499–509.
Kalicki, T., 2000. Grain size of the overbank deposits as carriers of paleogeographical information. Quat. Int. 72, 107–114.
Kalicki, T., Starkel, L., Sala, J., Soja, R., Zernickaya, V.P., 1996. Subboreal paleochannel system in the Vistula valley near Zabierzów Bocheński (Sandomierz Basin) (special issue). Geogr. Stud. (Wrocław) 9, 129–158.
Kalicki, T., Sauychyk, S., Calderoni, G., Simakova, G., 2008. Climatic versus human impact on the Holocene sedimentation in river valleys of different orded: examples from the upper Dnieper basin, Belarus. Quat. Int. 189, 91–105.
Kalis, A.J., Merkt, J., Wunderlich, J., 2003. Environmental changes during the Holocene climatic optimum in central Europe — human impact and natural causes. Quat. Sci. Rev. 22, 33–79.
Klimek, K., 2002. Human-induced overbank sedimentation in the foreland of the Eastern Sudety Mountains. Earth Surf. Process. Landf. 27 (4), 391–402.
Krejčí, O., Baroň, I., Bíl, M., Hubatka, F., Jurová, Z., Kirchner, K., 2002. Slope movements in the Flysch Carpathians of Eastern Czech Republic triggered by extreme rainfalls in 1997: a case study. Phys. Chem. Earth 27, 1567–1576.
Krumbein, W.C., Sloss, L.L., 1963. Stratigraphy and Sedimentation. Freeman, San Francisco.
Kukulak, J., 2000. Sedimentary record of early wood burning in alluvium of mountain streams in the Bieszczady range, Polish Carpathians. Palaeogeogr. Palaeoclimatol. Palaeoecol. 164, 167–175.
Kukulak, J., 2003. Impact of mediaeval agriculture on the alluvium in the San River headwaters (Polish Eastern Carpathians). Catena 51, 255–266.
Lamb, W.H., 1995. Climate, History and the Modern World, 2nd edition. Routledge, London.
Loke, M.H., 2012. Tutorial: 2-D and 3-D electrical imaging surveys. User's manual.Geotomo software, Penang.
Macaire, J.J., Bernard, J., Di-Giovanni, C., Hinschberger, F., Limondin-Lozouet, N., Visset, L., 2006. Quantification and regulation of organic and mineral sedimentation in a late-Holocene floodplain as a result of climatic and human impacts (Taligny marsh, Parisian Basin, France). The Holocene 16, 647–660.
Macklin, M.G., Lewin, J., 1993. Holocene river alluviation in Britain. Z. Geomorphol. Suppl. 88, 109–122.
Macklin, M.G., Lewin, J., 2003. River sediments, great floods and centennial-scale Holocene climate change. J. Quat. Sci. 18, 101–105.
Macklin, M.G., Benito, G., Gregory, K.J., Johnstone, E., Lewin, J., Michczyńska, D.J., Soja, JI, Starkel, L., Thorndycraft, V.R., 2006. Past hydrological events reflected in the Holocene fluvial record of Europe. Catena 66, 145–154.
Macoun, J., Šibrava, V., Tyráček, J., Kneblová-Vodičková, V., 1965. Kvartér Ostravska a Moravské Brány. Nakladatelství ČSAV, Praha.
Magny, M., 1993. Holocene fluctuations of lake levels in the French Jura and sub-Alpine ranges and their implications for past general circulation pattern. The Holocene 3, 306–313.
Magny, M., 2004. Holocene climate variability as reflectedby mid-European lake-level fluctuations and its probable impact on prehistoric human settlements. Quat. Int. 113, 65–79.
Magny, M., Leuzinger, U., Bortenschlager, S., Haas, J.N., 2006. Tripartite climate reversal in Central Europe 5600–5300 years ago. Quat. Res. 65, 3–19.
Mangerud, J., Andersen, S.T., Berglund, B.E., Donner, J.J., 1974. Quaternary stratigraphy of Norden, a proposal for terminology and classification. Boreas 3, 109–126.
Margielewski, W., 1997. Dated landslides of the Jaworzyna Krynicka Range (Outer Carpathians) and their relation to climatic phases of the Holocene. Ann. Soc. Geol. Pol. 67, 83–92.
Margielewski, W., 1998. Landslide phases in the Polish Outer Carpathians, and their relation to climatic changes in the Late Glacial and the Holocene. Quatern. Stud. Pol. 15, 37–53.
Margielewski, W., 2001. Late Glacial and Holocene climatic changes registered in forms and deposits of the Klaklowo landslide (Beskid Średni Range, Outer Carpathians). Stud. Geomorphol. Carpatho-Balc. 35, 63–79.
Margielewski, W., 2003. Late Glacial–Holocene palaeoenvironmental changes in the Western Carpathians: case studies of landslide forms and deposits. Folia Quat. 74, 1–96.
Margielewski, W., 2006. Records of the Late Glacial–Holocene palaeoenvironmental changes in landslide forms and deposits of the Beskid Makowski and Beskid Wyspowy Mts. Area (Polish Outer Carpathians). Folia Quaternaria 76, 1–149.
Margielewski, W., Kovalyukh, N.N., 2003. Neoholocene climatic changes recorded in landslide's peat bog on Mount Ćwilin (Beskid Wyspowy Range, Outer Carpathians). Stud. Geomorphol. Carpatho-Balc. 37, 59–76.
Margielewski, W., Krąpiec, M., Valde-Nowak, P., Zernitskaya, V., 2010. A Neolithic yew bow in the Polish Carpathians: Evidence of the impact of human activity on mountainous palaeoenvironment from the Kamiennik landslide peat bog. Catena 80, 141–153.
Margielewski, W., Kołaczek, P., Michczyński, A., Obidowicz, A., Pazdur, A., 2011. Record of the meso-and neoholocene palaeoenvironmental changes in the Jesionowa landslide peat bog (Beskid Sądecki Mts. Polish Outer Carpathians). Geochronometria 38, 138–154.
Menčík, E., 1983. Geologie Moravskoslezských Beskyd a Podbeskydské pahorkatiny. Academia, Praha.
Miall, A.D., 2006. The Geology of Fluvial Deposits: Sedimentary Facies, Basin Analysis and Petroleum Geology. Springer-Verlag, Berlin.
Milsom, J., 2005. Field Geophysics, the Geological Field Guide Series. Wiley, Chichester.
Morin, E., Macaire, J.J., Hinschberger, F., Gay-Ovéréjo, I., Rodrigues, S., Bakyono, J.P., Visset, L., 2011. Spatio-temporal evolution of the Choisille River (southern Parisian Basin, France) during the Weichselian and the Holocene as a record of climate trend and human activity in north-western Europe. Quat. Sci. Rev. 30, 347–363.
Nanson, G.C., Croke, J.C., 1992. A genetic classification of floodplains. Geomorphology 4, 459–486.
Nehyba, S., Nývlt, D., Schkade, U., Kirchner, G., Franců, E., 2011. Depositional rates and dating techniques of modern deposits in the Brno reservoir (Czech Republic) during the last 70 years. J. Paleolimnol. 45, 41–55.
Niggemann, S., Mangini, A., Mudelsee, M., Richter, D.K., Wurth, G., 2003. Sub-Milankovitch climatic cycles in Holocene stalagmites from Sauerland, Germany. Earth Planet. Sci. Lett. 216, 539–547.
Notebaert, B., Verstraeten, G., 2010. Sensitivity of West and Central European river systems to environmental changes during the Holocene: A review. Earth Sci. Rev. 103, 163–182.
Novák, M., Emmanuel, S., Vile, M.A., Erel, Y., Véron, A., Pačes, T., Wieder, K.R., Vaněček, M., Štěpánová, M., Břízová, E., Hovorka, J., 2003. Origin of lead in eight central European peat bogs determined from isotope ratios, strengths, and operation times of regional pollution sources. Environ. Sci. Technol. 37, 437–445.
Opravil, E., 1974. Moravskoslezský pomezní les do počátku kolonizace. Archeol. Sb. 1, 113–131.
Owens, P.N., Walling, D.E., Leeks, G.J.L., 1999. Use of floodplain sediment cores to investigate recent historical changes in overbank sedimentation rates and sediment sources in the catchment of the River Ouse, Yorkshire, UK. Catena 36, 21–47.
Pánek, T., Smolková, V., Hradecký, J., 2010. Reconstruction of a Holocene average catchment denudation from the landslide-dammed lakes in the Outer Western Carpathians. EGU General Assembly 2010, Vienna. Geophysical Research Abstracts, 12.
Pánek, T., Smolková, V., Hradecký, J., Sedláček, J., Zernitskaya, V., Kadlec, J., Pazdur, A., Řehánek, T., 2013a. Late-Holocene evolution of a floodplain impounded by the Smrdutá landslide, Carpathian Mountains (Czech Republic). The Holocene 23, 218–229.
Pánek, T., Smolková, V., Hradecký, J., Baroň, I., Šilhán, K., 2013b. Holocene reactivations of catastrophic complex flow-like landslides in the Flysch Carpathians (Czech Republic/Slovakia). Quat. Res. 80, 33–46.
Podborský, V., Čižmář, M., Dvořák, P., Erhart, A., Janák, V., Medunová-Benešová, A., Nekvasil, J., Ondráček, J., Pavelčík, J., Podhorský, V., Salaš, M., Stuchlík, S., Stuchlíková, J., Šebela, L., Šmíd, M., Strof, A., Tejral, J., Valoch, K., 1993. Pravěké dějiny Moravy. Muzejní a vlastivědná společnost v Brně, Brno.
Ralska-Jasiewiczowa, M., 1980. Late Glacial and Holocene of the Bieszczady Mountains (Polish eastern Carpathians). PWN, Warszawa.
Ramsey, C.B., 2007. Radiocarbon Calibration and Analysis of Stratigraphy: the OxCal Program 4.0.5. http://c14.arch.ox.ac.uk/embed.php?File=oxcal.html (last accessed March 2013).
Reimer, P.J., Baillie, M.G.L., Bard, E., Bayliss, A., Beck, J.W., Blackwell, P.G., Bronk Ramsey, C., Buck, C.E., Burr, G.S., Edwards, R.L., Friedrich, M., Grootes, P.M., Guilderson, T.P., Hajdas, I., Heaton, T.J., Hogg, A.G., Hughen, K.A., Kaiser, K.F., Kromer, B., McCormac, F.G., Manning, S.W., Reimer, R.W., Richards, D.A., Southon, J.R., Talamo, S., Turney, C.S.M., van der Plicht, J., Weyhenmeyer, C.E., 2009. IntCal09 and Marine09 radiocarbon age calibration curves, 0–50,000 years cal BP. Radiocarbon 51 (4), 1111–1150.
Reineck, H.E., Singh, I.B., 1980. Depositional Sedimentary Environments, second ed. Springer-Verlag, Berlin.
Rodenburg, J., Stein, A., van Noordwijk, M., Ketterings, Q.M., 2003. Spatial variability of soil pH and phosphorus in relation to soil run-off following slash-and-burn land clearing in Sumatra, Indonesia. Soil Tillage Res. 71, 1–14.

Schenk, Z., 2004. Nejstarší neolitické osídlení jihozápadní části Moravské brány (K problematice osídlení přerovského regionu v období kultury s lineární keramikou). Sborník Státního okresního archivu v Přerově. 6–41.
Šebela, L., Pavelčík, J., Beneš, J., Dočkalová, M., Furholt, M., Gregor, M., Kratochvíl, Z., Komárková, V., Nývltová Fišáková, M., Opravil, E., Přichystal, A., Schenk, Z., Škrdla, P., 2007. Hlinsko: výšinná osada lidu Badenské kultury. Archeologický ústav AV ČR, Brno.
Sedláček, J., Bábek, O., Grygar, T., 2013. Trends and evolution of contamination in a well-dated water reservoir sedimentary archive: the Brno Dam, Moravia, Czech Republic. Environ. Earth Sci. 69 (8), 2581–2593.
Smolková, V., 2011. Slope Deformations and their Impact on Valley Bottom Development (in the Czech Part of the Carpathians). (PhD thesis) University of Ostrava, Ostrava.
Smolková, V., Pánek, T., Hradecký, J., 2008. Fossil landslide-dammed lake in the Babínek valley (Vsetínské vrchy Hills): contribution to understanding the Holocene relief development in the flysch Carpathians. Geol. výzk. Mor. Slezsku roce 2007 (15), 41–43.
Starkel, L., 1995. New data on the Late Vistulian and Holocene evolution of the Wisłoka River valley near Dębica. In: Starkel, L. (Ed.), Evolution of the Vistula River valley during the last 15000 years, part V. Geographical Studies, Special Issue, 8. IGiPZPAN, pp. 73–90.
Starkel, L., Soja, R., Michczynska, D.J., 2006. Past hydrological events reflected in Holocene history of Polish rivers. Catena 66, 24–33.
Starkel, L., Gębica, P., Superson, J., 2007. Last Glacial–Interglacial cycle in the evolution of river valleys in southern and central Poland. Quat. Sci. Rev. 26, 2924–2936.
Štika, J., 2007. Valaši a Valašsko: o původu Valachů, valašské kolonizaci, vzniku a historii moravského Valašska a take karpatských salaších. Valašské museum v přírodě, Rožnov pod Radhoštěm.
Tolasz, R. (Ed.), 2007. Climate atlas of Czechia. Czech Hydrometeorological Institute, Prague.
Turner, F., Tolksdorf, J.F., Viehberg, F., Schwalb, A., Kaiser, K., Bittmann, F., von Bramann, U., Pott, R., Staesche, U., Breest, K., Veil, S., 2013. Lateglacial/early Holocene fluvial reactions of the Jeetzel river (Elbe valley, northern Germany) to abrupt climatic and environmental changes. Quat. Sci. Rev. 60, 91–109.
Tyráček, J., 1963. On the problem of the parallelization of the continental and alpine glaciation on the territory of Czechoslovakia. Report of the VIth INQUA Congress, 3, pp. 375–384.
Vít, J., Kolář, T., Rybníček, M., 2009. Preliminary results of the relations between subfossil trunks and fluvial sediments on Osek nad Bečvou and Tovačov-Annín localities. Geol. výzk. Mor. Slezsku 16, 53–55.
Wanner, H., Beer, J., Bütikofer, J., Crowley, T.J., Cubasch, U., Flückiger, J., Goosse, H., Grosjean, M., Joos, F., Kaplan, J.O., Küttel, M., Müller, S.A., Prentice, I.C., Solomina, O., Stocker, T.F., Tarasov, P., Wagner, M., Widmann, M., 2008. Mid- to late Holocene climate change — an overview. Quat. Sci. Rev. 27, 1791–1828.
Wildi, W., Dominik, J., Loizeau, J.L., Thomas, R.L., Favarger, P.Y., Haller, L., Perroud, A., Peytremann, C.H., 2004. River, reservoir and lake sediments contamination by heavy metals downstream from urban areas of Switzerland. Lake Reserv. Manag. 9, 75–87.
Záruba, Q., 1922. Study on landslide terrains in the Vsetín and Vallachian Region. Práce z geologického ústavu čes.vys. učení technického v Praze 170–177.
Zygmunt, E., 2004. Archaeological and radiocarbon dating of alluvial fans as an indicator of prehistoric colonisation of the Głubczyce Plateau (Southwestern Poland). Geochronometra 23, 101–107.